

Ligand-Dependent Catalytic Cycle and Role of Styrene in Nickel-Catalyzed Anhydride Cross-Coupling: Evidence for Turnover-Limiting Reductive Elimination

Jeffrey B. Johnson,[†] Eric A. Bercot,[†] John M. Rowley,[‡] Geoffrey W. Coates,[‡] and Tomislav Rovis^{*†}

Contribution from Colorado State University, Fort Collins, Colorado 80523, and the Department of Chemistry and Chemical Biology, Baker Laboratory, Cornell University, Ithaca, New York 14853

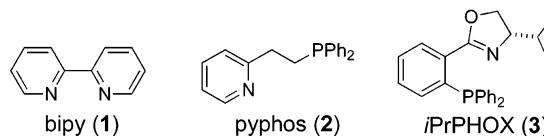
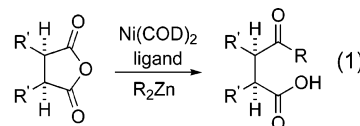
Received November 2, 2006; E-mail: rovis@lamar.colostate.edu

Abstract: Results from a mechanistic study on the Ni(COD)₂-bipy-catalyzed alkylation of anhydrides are consistent with turnover-limiting reductive elimination at high Et₂Zn concentrations. While the presence of styrene does not affect the initial rate of alkylation, it appears to inhibit catalyst decomposition and provides higher product yield at long reaction times. In contrast, Ni(COD)₂-*i*-PrPHOX-catalyzed anhydride alkylation proceeds through two competing catalytic cycles differentiated by the presence of styrene. The presence of styrene in this system appears to accelerate rate-limiting oxidative addition and promotes the cycle which proceeds 4 times more rapidly and with much higher enantioselectivity than its styrene-lacking counterpart.

Introduction

Metal-catalyzed cross-coupling reactions have revolutionized methods through which molecules are assembled.¹ Despite the success of transition metal-catalyzed cross-coupling, frontiers remain in this area, including the use of sp³ coupling partners and the challenge of introducing or defining stereochemistry. Although a wide variety of activated acyl species have been utilized in the formation of ketones, anhydrides have only recently been investigated as acylating agents in metal-mediated reactions.² The Rovis group, among others,³ has been engaged in the development of cross-coupling reactions of carboxylic anhydrides. We have discovered the alkylation of cyclic anhydrides with organozinc nucleophiles, catalyzed by nickel species, which produces 1,4- or 1,5-ketoacids (eq 1). Both bidentate N,N and P,N ligands have been utilized, with optimal

yields of the desired ketoacids provided in high yields by bipyridine (bipy, **1**) for succinic anhydrides and pyphos (**2**) for glutaric anhydrides.⁴ The power of this methodology lies in the ability to transform cyclic carboxylic anhydrides into ketoacid derivatives with stereodefined backbones. While excellent enantioselectivities have been realized for succinic anhydrides using a similar palladium-catalyzed system,⁵ the desymmetrization of glutaric anhydrides has generally resulted in moderate enantioselectivities,⁶ the best of which are observed with Ni(COD)₂ and isopropyl-phosphinooxazoline (*i*-PrPHOX, **3**).



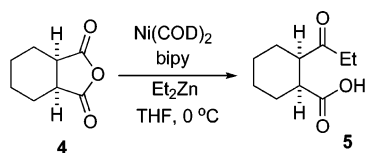
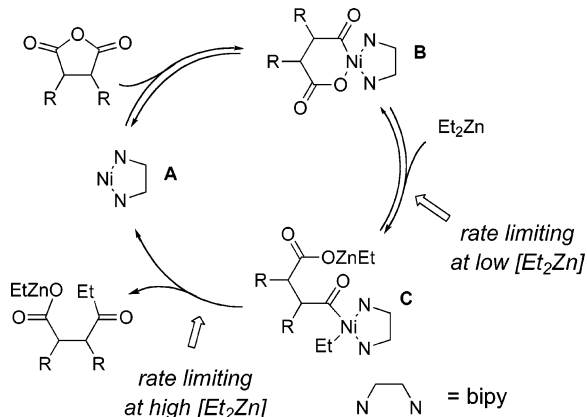
Mechanistic studies are typically conducted with the aim of better understanding the underlying processes in an effort to address current deficiencies. Within the field of carbon-carbon bond-forming couplings, however, relatively few have focused upon the full catalytic process.⁷ While kinetic details are greatly dependent upon the specific system under investigation, either

[†] Colorado State University.

[‡] Cornell University.

- (1) Diederich, F.; Stang, P. J. *Metal-Catalyzed Cross-Coupling Reactions*; Wiley-VCH: Weinheim, 1998.
- (2) Use of acid chlorides: (a) Kosugi, M.; Shimizu, Y.; Migita, T. *Chem. Lett.* **1977**, 1423. (b) Milstein, D.; Stille, J. K. *J. Am. Chem. Soc.* **1978**, *100*, 3636. (c) Milstein, D.; Stille, J. K. *J. Org. Chem.* **1979**, *44*, 1613. Thioesters: (d) Tokuyama, H.; Yokoshima, S.; Yamashita, T.; Fukuyama, T. *Tetrahedron Lett.* **1998**, *39*, 3189. (e) Liebeskind, L. S.; Srogl, J. *J. Am. Chem. Soc.* **2000**, *122*, 11260. (f) Wittenberg, R.; Srogl, J.; Egi, M.; Liebeskind, L. S. *Org. Lett.* **2003**, *5*, 3033. Aryl trifluoroacetates: (g) Kakino, R.; Shimizu, I.; Yamamoto, A. *Bull. Chem. Soc. Jpn.* **2001**, *74*, 371. Acyl cyanides: (h) Duplais, C.; Bures, F.; Sapountzis, I.; Korn, T. J.; Cahiez, G.; Knochel, P. *Angew. Chem., Int. Ed.* **2004**, *43*, 2968. Acid fluorides: (i) Zhang, Y.; Rovis, T. *J. Am. Chem. Soc.* **2004**, *126*, 15964.
- (3) (a) Real, S. D.; Kronenthal, D. R.; Wu, H. Y. *Tetrahedron Lett.* **1993**, *34*, 8063. (b) Goossen, L. J.; Ghosh, K. *Angew. Chem., Int. Ed.* **2001**, *40*, 3458. (c) Frost, C. G.; Wadsworth, K. J. *Chem. Commun.* **2001**, 2316. (d) Kakino, R.; Yasumi, S.; Shimizu, I.; Yamamoto, A. *Bull. Chem. Soc. Jpn.* **2002**, *75*, 137. (e) Wang, D.; Zhang, Z. *Org. Lett.* **2003**, *5*, 4645. (f) Hong, Y.-T.; Barchuk, A.; Krische, M. J. *Angew. Chem., Int. Ed.* **2006**, *45*, 6885. (g) For a complementary approach, see: Shintani, R.; Fu, G. C. *Angew. Chem., Int. Ed.* **2002**, *41*, 1057.

- (4) (a) Bercot, E. A.; Rovis, T. *J. Am. Chem. Soc.* **2002**, *124*, 174. (b) Bercot, E. A.; Rovis, T. *J. Am. Chem. Soc.* **2005**, *127*, 247. (c) Johnson, J. B.; Yu, R. T.; Fink, P.; Bercot, E. A.; Rovis, T. *Org. Lett.* **2006**, *8*, 4307.
- (5) Bercot, E. A.; Rovis, T. *J. Am. Chem. Soc.* **2004**, *126*, 10248.
- (6) Bercot, E. A. Ph.D. Thesis. Colorado State University, 2004.

Scheme 1. Reaction Utilized for the Mechanistic Study**Scheme 2.** Proposed Catalytic Cycle for the Alkylation of Anhydrides with Et_2Zn Catalyzed by $\text{Ni}(\text{COD})_2$ and bipy

oxidative addition or transmetalation is typically the turnover-limiting step of catalysis. Although a single example of rate-limiting reductive elimination has been proposed,⁸ no detailed kinetic studies have been reported to support this hypothesis. To address current shortcomings in our newly developed methodology, we initiated a mechanistic study to determine the catalytic cycle. Herein we report the results of this study, including a description of the catalytic cycle and its dependence upon the ligand, bipy or ⁱPrPHOX, and an outline of the different role of styrene in each system.

Results and Discussion

Our study began with the investigation of the alkylation of *cis*-1,2-cyclohexanedicarboxylic anhydride (**4**). In situ IR spectroscopy was utilized to monitor the reaction, which was carried out with diethyl zinc, catalyzed by $\text{Ni}(\text{COD})_2$ and bipy (Scheme 1).⁹ The alkylation reaction is typically carried out in the presence of 4-fluorostyrene, as the presence of this additive provides qualitatively higher yields and shorter reaction times.^{6,4b} Addition of styrene has previously been utilized by Knochel, who proposed that styrene accelerates cross-coupling reactions by facilitation of reductive elimination.^{8,10} Due to apparent mixed kinetic dependences observed at full reaction time, the method of initial rates was used to determine the reaction rate.

Kinetic Study. Variation of the concentration of each reaction component and compilation of the corresponding rate data resulted in the determination of the kinetic rate law. This

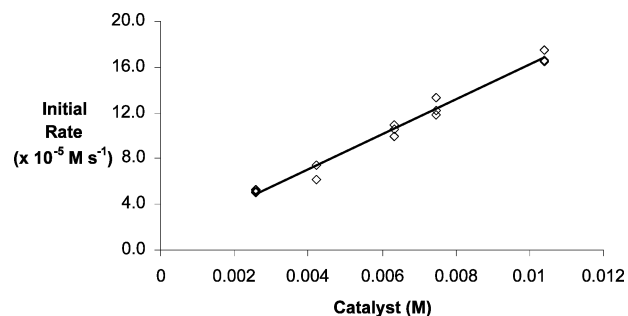


Figure 1. Plot of initial rate of anhydride (**4**) alkylation versus the concentration of $[\text{Ni}(\text{COD})_2/\text{bipy}]$ (1:1.1 ratio): $[\text{4}] = 0.10 \text{ M}$, $[\text{4-F-styrene}] = 16 \text{ mM}$, $[\text{Et}_2\text{Zn}] = 0.15 \text{ M}$ at 0°C .

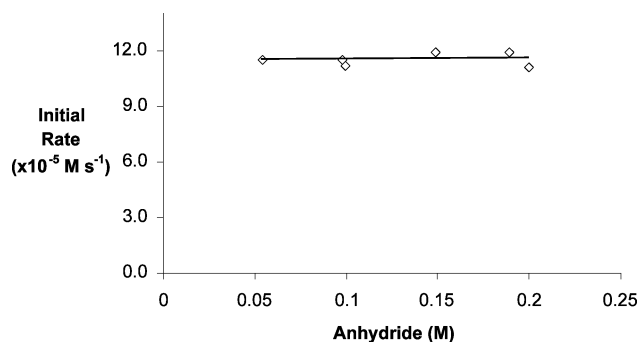


Figure 2. Plot of initial rate of anhydride (**4**) alkylation versus the concentration of **4**: $[\text{Ni}(\text{COD})_2] = 7.7 \text{ mM}$, $[\text{bipy}] = 8.2 \text{ mM}$, $[\text{4-F-styrene}] = 16 \text{ mM}$, $[\text{Et}_2\text{Zn}] = 0.15 \text{ M}$ at 0°C .

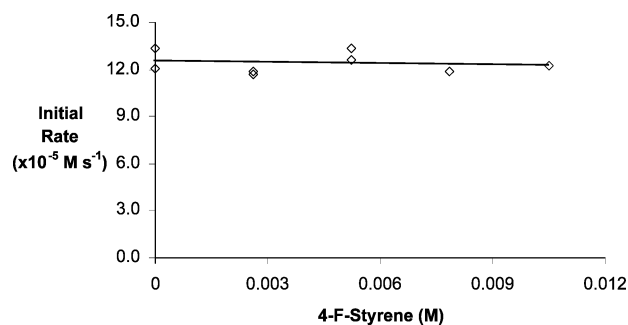


Figure 3. Plot of initial rate of anhydride (**4**) alkylation versus the concentration of 4-fluorostyrene: $[\text{Ni}(\text{COD})_2] = 7.7 \text{ mM}$, $[\text{bipy}] = 8.2 \text{ mM}$, $[\text{Et}_2\text{Zn}] = 0.15 \text{ M}$, $[\text{4}] = 0.10 \text{ M}$ at 0°C .

information led to the proposed catalytic cycle (Scheme 2). The reaction rate displays first-order dependence on catalyst (Figure 1),¹¹ but zero-order dependence upon anhydride **4** (Figure 2). The initial rate is also independent of 4-F-styrene under all concentrations, including the complete absence of styrene (Figure 3). Variation of Et_2Zn concentration results in nearly first-order behavior at low concentrations, but little to no dependence at concentrations above 0.14 M (Figure 4). This saturation behavior observed with variation of Et_2Zn concentration indicates a shift in the turnover-limiting step. This observation is consistent with turnover-limiting transmetalation at low Et_2Zn concentrations. At higher concentrations of Et_2Zn the second-order process of transmetalation proceeds more rapidly, resulting in an equilibrium between intermediates **B** and **C** (Scheme 2). Reductive elimination, a first-order process that does not significantly accelerate with increasing Et_2Zn concentration, becomes rate

(7) For leading references, see: (a) Amatore, C.; Jutand, A. *J. Organomet. Chem.* **1999**, *576*, 254. (b) Espinet, P.; Echavarren, A. M. *Angew. Chem., Int. Ed.* **2004**, *43*, 4704. (c) Frisch, A. C.; Beller, M. *Angew. Chem., Int. Ed.* **2005**, *44*, 674. (d) Denmark, S. E.; Sweis, R. F. *J. Am. Chem. Soc.* **2004**, *126*, 4876. (e) Anderson, T. J.; Jones, G. D.; Vivic, D. A. *J. Am. Chem. Soc.* **2004**, *126*, 8100. (f) Trost, B. M. *J. Org. Chem.* **2004**, *69*, 5813. (g) Belda, O.; Moberg, C. *Acc. Chem. Res.* **2004**, *37*, 159. (h) Jones, G. D.; Martin, J. L.; McFarland, C.; Allen, O. R.; Hall, R. E.; Haley, A. D.; Brandon, R. J.; Kononova, T.; Desrochers, P. J.; Pulay, P.; Vivic, D. A. *J. Am. Chem. Soc.* **2006**, *128*, 13175.

(8) Giovannini, R.; Knochel, P. *J. Am. Chem. Soc.* **1998**, *120*, 11186.

(9) No reaction between **4** and Et_2Zn is observed in the absence of $\text{Ni}(\text{COD})_2$.

(10) (a) Giovannini, R.; Stüdemann, T.; Dussin, G.; Knochel, P. *Angew. Chem., Int. Ed.* **1998**, *37*, 2387. (b) Giovannini, R.; Stüdemann, T.; Devasagayaraj, A.; Dussin, G.; Knochel, P. *J. Org. Chem.* **1999**, *64*, 3544.

(11) The intercept of this plot is $0.4 \times 10^{-5} \text{ M s}^{-1}$. Independent studies have shown that in the absence of $\text{Ni}(\text{COD})_2$, no reaction occurs between Et_2Zn and **4** after 6 h at room temperature. See ref 4b.

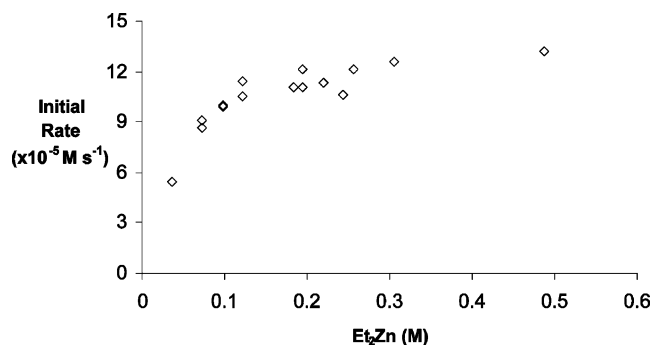


Figure 4. Plot of initial rate of anhydride (**4**) alkylation versus the concentration of Et₂Zn: [4] = 0.10 M, [Ni(COD)₂] = 7.7 mM, [bipy] = 8.2 mM, [4-F-styrene] = 16 mM at 0 °C.

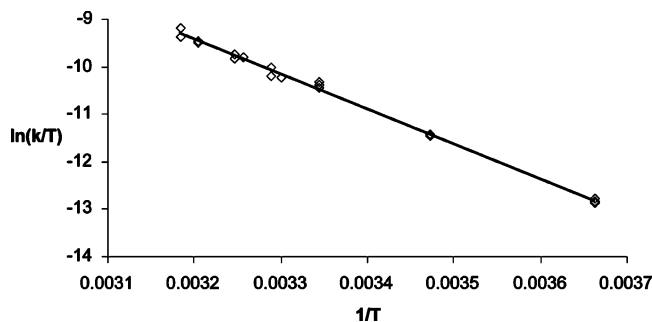


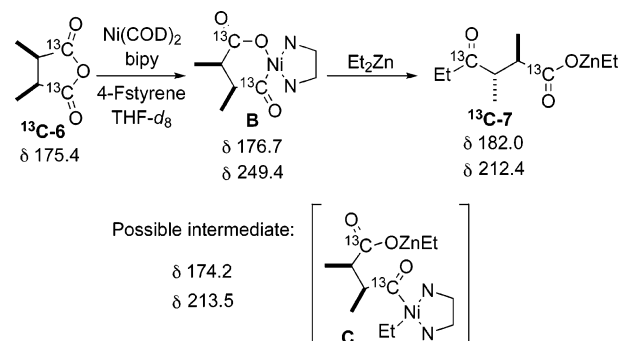
Figure 5. Eyring plot constructed from the rate constants determined from the initial rate of alkylation of **4** with Et₂Zn at temperatures between 0 and 41 °C.

limiting under these conditions. This represents an unusual turnover-limiting step for catalytic cross-coupling and is particularly rare for the formation of carbon–carbon bonds.¹²

Determination of Activation Parameters. To further probe the nature of the anhydride alkylation, the temperature dependence of the reaction was explored. Initial rates for the alkylation of **4** with Et₂Zn were determined for reactions performed between 0 and 41 °C, using standard reaction conditions: [4] = 0.10 M, [Et₂Zn] = 0.15 M, [Ni(COD)₂] = 7.8 mM, [bipy] = 8.0 mM, [4-F-styrene] = 15.7 mM. From the data reported above, the rate law under these conditions is first order in catalyst and zero order in both Et₂Zn and **4**, and the rate constants were determined as such. The resulting rate constants were utilized to construct an Eyring plot (Figure 5), which provides activation parameters of $\Delta H^\ddagger = 14.7 \pm 2.4$ kcal/mol and $\Delta S^\ddagger = -18.8 \pm 3.8$ eu.

Examination of the Resting State. The reaction was further examined using ¹³C-labeled 2,3-dimethylsuccinic anhydride (¹³C-**6**).¹³ Addition of 1 equiv of Ni–bipy and 2 equiv of 4-fluorostyrene to 5 equiv of ¹³C-**6** allowed the observation of resonances consistent with intermediate **B** by ¹³C NMR spectroscopy (δ 176.7 and 249.4 at –60 °C in THF-*d*₈) (Scheme 3).¹⁴ Subsequent addition of a large excess (35 equiv) of Et₂Zn

Scheme 3. Synthesis of Intermediate **B** and Tentative Assignment of Intermediate **C** by ¹³C NMR Spectroscopy



at –45 °C resulted in several changes to the solution. Resonances corresponding to labeled anhydride ¹³C-**6** were still visible, and those from product ¹³C-**7** slowly appeared. More importantly, resonances corresponding to intermediate **B** disappeared, and new resonances corresponding to a transient species were observed at δ 174.2 and 213.5. These transient peaks, which disappeared as the reaction reached completion, are tentatively proposed to correspond to intermediate **C** (Scheme 3).^{15,16}

Reversible Oxidative Addition. Despite the absence of anhydride **4** from the rate law, it is proposed that initial oxidative addition is fast and reversible, as the oxidative addition products are readily observed upon addition of an anhydride to a Ni–bipy solution.¹⁷ We reasoned that if the equilibrium of **A** and **B** strongly favors **B** (Scheme 2), then additional anhydride does not significantly increase its equilibrium concentration and thus results in no change in the initial rate. Support for this proposal was obtained with a stoichiometric experiment. The oxidative addition complex of Ni(COD)₂–bipy with anhydride **4**, prepared by addition of 1 equiv of **4** to 1 equiv of Ni(COD)₂ and bipy in the presence of 2 equiv of 4-F-styrene, was treated with 1 equiv of *cis*-2,3-dimethyl succinic anhydride (**6**) and 0.9 equiv of Et₂Zn (Figure 6).¹⁸ Upon workup, ketoacids **5** and **7**, derived from **4** and **6**, respectively, were obtained in a 1.5:1 ratio. Isolation of both products clearly indicates that oxidative addition is reversible. When the order of addition was reversed, products **5** and **7** were obtained in a 1.3:1 ratio, further supporting this conclusion. Observation of reversible oxidative addition suggests that at low anhydride concentrations, beyond the detection limits of our instrumentation, first-order rate dependence would be observed.

Styrene Effect. Also noteworthy is the absence of 4-F-styrene from the rate law, despite rate-limiting reductive elimination at

- (12) Pflötzschner, T.; Kleeman, L.; Janza, B.; Harms, K.; Schrader, T. *Chem. Eur. J.* **2004**, *10*, 6048. Other systems with rate-limiting reductive elimination: C–H bond formation: (a) Halpern, J. *Asymmetric Synthesis*; Academic Press: New York, 1983; Vol 5, p 48. C–S bond formation: (b) Moreau, X.; Campagne, J. M.; Meyer, G.; Jutand, A. *Eur. J. Org. Chem.* **2005**, 3749.
- (13) (a) Rowley, J. M.; Lobkovsky, E. B.; Coates, G. W. *J. Am. Chem. Soc.*, in press. (b) Getzler, Y. D. Y. L.; Kundnani, V. K.; Lobkovsky, E. B.; Coates, G. W. *J. Am. Chem. Soc.* **2004**, *126*, 6842.
- (14) Other acyl–nickel ¹³C NMR data: (a) Schultz, C. S.; DeSimone, J. M.; Brookhart, M. *J. Am. Chem. Soc.* **2001**, *123*, 9172. (b) Schultz, C. S.; DeSimone, J. M.; Brookhart, M. *Organometallics* **2001**, *20*, 16.

- (15) See Supporting Information for full reaction details and ¹³C NMR spectra. When a similar reaction is carried out in the absence of 4-fluorostyrene, no appreciable difference in the ¹³C NMR spectrum is observed.
- (16) To the best of our knowledge, there have been no reports of isolated Ni–acyl–alkyl species. Several reports have appeared of isolated compounds that form ketones upon treatment with another reagent, presumably through such an intermediate. Grignard addition to a Ni(II)–acyl species; see: (a) Saruyama, T.; Yamamoto, T.; Yamamoto, A. *Bull. Chem. Soc. Jpn.* **1976**, *49*, 546. (b) Stoppioni, P.; Dapporto, P.; Sacconi, L. *Inorg. Chem.* **1978**, *17*, 718. Formation of ketones from CO insertion into a Ni(II)–dialkyl complex; see: (c) Yamamoto, T.; Kohara, T.; Yamamoto, A. *Chem. Lett.* **1976**, 1217. (d) Yamamoto, T.; Kohara, T.; Yamamoto, A. *Bull. Chem. Soc. Jpn.* **1981**, *54*, 2161.
- (17) (a) Uhlig, E.; Fehske, G.; Nestler, B. Z. *Anorg. Allg. Chem.* **1980**, 465, 141. (b) Komiya, S.; Yamamoto, A.; Yamamoto, Y. *Chem. Lett.* **1981**, 193. (c) Sano, K.; Yamamoto, T.; Yamamoto, A. *Bull. Chem. Soc. Jpn.* **1984**, *57*, 2741.
- (18) We have yet to successfully isolate a metallacycle corresponding to intermediate **B**.

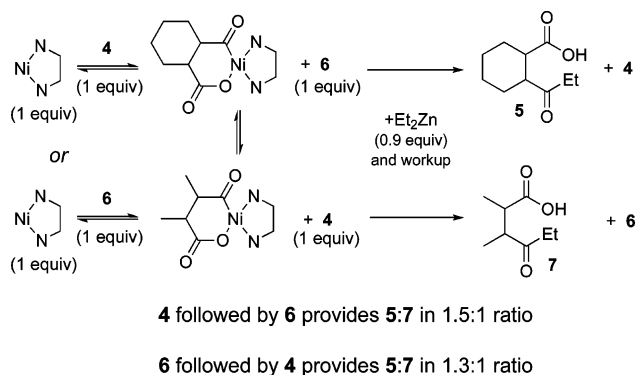


Figure 6. Experiment testing reversibility of oxidative addition.

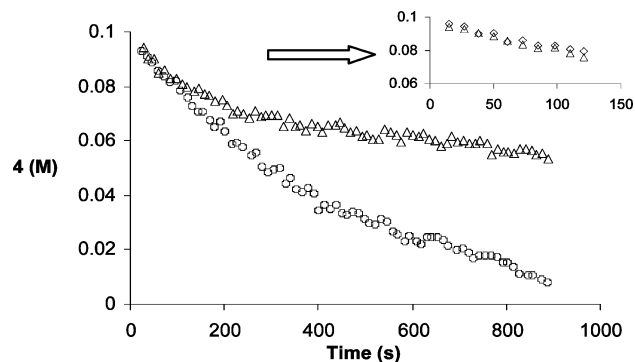
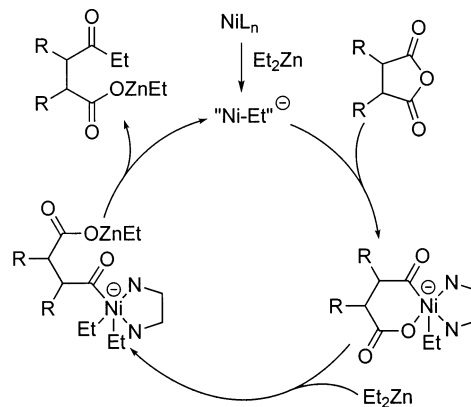


Figure 7. Plot of anhydride **4** concentration versus time with 0.016 M 4-F-styrene (O) and without (Δ) styrene: $[\text{Ni}(\text{COD})_2] = 7.1 \text{ mM}$, $[\text{bipy}] = 7.9 \text{ mM}$, $[\mathbf{4}] = 0.10 \text{ M}$, $[\text{Et}_2\text{Zn}] = 0.15 \text{ M}$. Inset shows magnification of first 20% of anhydride consumption.

high Et_2Zn concentration. Although the initial rates are identical to 15% conversion, the inclusion of styrene results in more rapid complete consumption of anhydride and higher ketoacid yields than reactions run in its absence. Investigation of the full reaction by in situ IR spectroscopy displays a gradual retardation of product formation in the absence of styrene (Figure 7). Conversion ends prior to complete anhydride consumption, implying a catalyst degradation pathway which is inhibited by the styrene.¹⁹ To address the possibility of rate retardation due to product inhibition, the reaction was performed in the presence of 1 equiv of the zinc ketocarboxylate. The reaction rates through 50% conversion were nearly identical in reactions in the presence and absence of product, both in the presence and absence of styrene, indicating that product inhibition does not significantly contribute to the observed rate retardation.

Complete Catalytic Cycle. The results of this series of studies are in all regards consistent with a system in which, at high concentrations of Et_2Zn , catalyst turnover is limited by reductive elimination. Reversible oxidative addition of the anhydride to the metal center suggests that oxidative addition occurs prior to the turnover-limiting step of the catalytic cycle. The saturation behavior observed upon variation of the Et_2Zn concentration clearly indicates a change in rate-limiting step, from transmetalation (presumably a second-order process that is first order in Et_2Zn concentration) to a subsequent unimolecular step which is independent of the concentration of Et_2Zn . This combination of observations indicates that reductive elimination is the turnover-limiting reaction in the catalytic

Scheme 4. Ni–Ethyl Complex Catalytic Cycle



alkylation of 1,2-cyclohexanedicarboxylic anhydride (**4**) with Et_2Zn .

One remaining mechanistic possibility involves the reversible formation of an Et_2Zn –nickel metallacycle coordination complex prior to transmetalation. This case would also result in saturation behavior, as complexation would limit catalyst turnover at low Et_2Zn concentrations, whereas transmetalation would become rate limiting at high concentrations. Evidence against this case is the relative rates of alkylation with Et_2Zn and Ph_2Zn . Formation of a R_2Zn –Ni complex is expected to be faster with the more Lewis-acidic Ph_2Zn than with Et_2Zn , yet alkylation with Ph_2Zn occurs more slowly. Furthermore, the lack of precedent for the rate-limiting formation of such a complex, in both stoichiometric and catalytic studies involving rate-limiting transmetalation, suggests that this situation is unlikely.²⁰

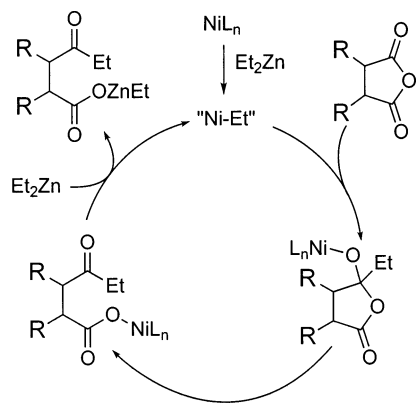
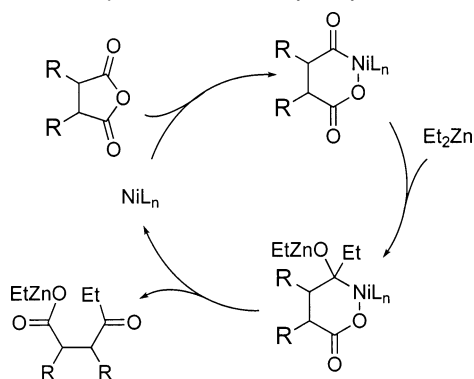
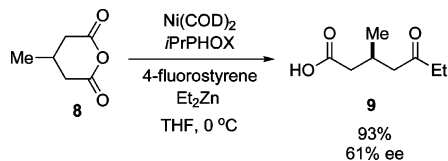
An additional mechanistic variation, based upon the active nickel species, may also be possible. The active catalytic species, currently proposed as a neutral nickel species, may conceivably be a nickel-ate complex. The reaction sequence may proceed as proposed, only through an anionic manifold. Reductive elimination is expected to be relatively slow from an electron-rich intermediate (Scheme 4).

Two other mechanisms have also been considered. If Ni–bipy reacts with Et_2Zn , forming a Ni–Et complex, this compound may subsequently add to one carbonyl of the anhydride (Scheme 5). Subsequent opening of the anhydride, followed by transmetalation, closes the catalytic cycle. This mechanism can be ruled out, however, as no reaction is observed upon addition of Et_2Zn to a solution of Ni–bipy in the absence of anhydride. Furthermore, this mechanism cannot adequately account for the zero-order anhydride dependence and the saturation kinetics observed upon variation of Et_2Zn concentration.

A mechanism consisting of oxidative addition followed by nucleophilic attack of Et_2Zn to the metallacycle must also be considered. Such a mechanism is provided in Scheme 6. Following Et_2Zn addition, the complex rearranges, providing the zinc carboxylate and closing the catalytic cycle. This mechanism is consistent with all kinetic data, in which nucleo-

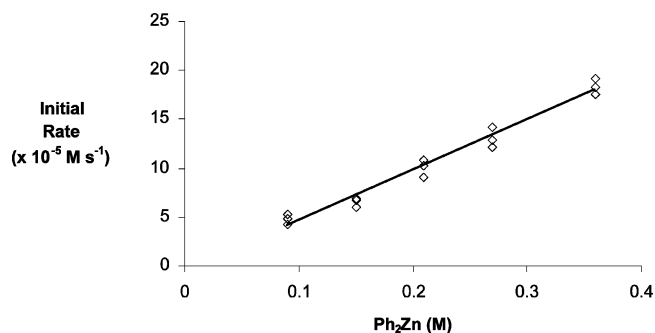
(19) Scriveranti, A.; Beghetto, V.; Matteoli, U.; Antonaroli, S.; Marini, A.; Crociani, B. *Tetrahedron* **2005**, *61*, 9752.

(20) For leading references, see: Osakada, K.; Yamamoto, T. *Coord. Chem. Rev.* **2000**, *198*, 379. See also: (a) Labadie, J. W.; Stille, J. K. *J. Am. Chem. Soc.* **1983**, *105*, 6129. (b) Grisso, B. A.; Johnson, J. R.; Mackenzie, P. B. *J. Am. Chem. Soc.* **1992**, *114*, 5160. (c) Farina, V.; Kapadia, S.; Krishnan, B.; Wang, C.; Liebeskind, L. S. *J. Org. Chem.* **1994**, *59*, 5905. (d) Denmark, S. E.; Sweis, R. F.; Wehrli, D. *J. Am. Chem. Soc.* **2004**, *126*, 4865. (e) Denmark, S. E.; Sweis, R. F. *J. Am. Chem. Soc.* **2004**, *126*, 4876.

Scheme 5. Ni–Ethyl Complex Catalytic Cycle**Scheme 6.** Nucleophilic Addition Catalytic Cycle**Scheme 7.** Desymmetrization of 4-Methyl Glutaric Anhydride **8** with Et₂Zn Catalyzed by Ni(COD)₂ and ⁱPrPHOX in the Presence of 4-Fluorostyrene

philic attack is rate limiting under low Et₂Zn concentrations and the rearrangement is rate limiting at higher concentrations. The data which eliminates this mechanism, however, is the observation of the transient species by ¹³C NMR spectroscopy under catalytic conditions. The resonances at 174.2 and 213.5 are not consistent with carboxylate and an sp³ hybridized carbon, thus suggesting that this mechanism is not in operation.

Change in Cycle with Diphenylzinc. It should be noted, however, that turnover-limiting reductive elimination is dependent upon the nature of the diorganozinc reagent. The arylation of **4** with Ph₂Zn proceeds at a slower initial rate ($6.5 \times 10^{-5} \text{ M s}^{-1}$) than alkylation with Et₂Zn ($11.2 \times 10^{-5} \text{ M s}^{-1}$) under identical conditions at low diorganozinc concentrations (0.10 M **4**, 0.15 M R₂Zn, 7.35 mM Ni(COD)₂, 7.92 mM bipy, 15.7 mM 4-F-styrene). In order to probe this reaction, the concentration of Ph₂Zn was increased, and its effect on the initial rate of reaction was observed. Up to 0.36 M Ph₂Zn, well above the saturation concentration for Et₂Zn, the reaction maintained its first-order dependence upon Ph₂Zn concentration (Figure 8). This suggests that when using diarylzinc nucleo-

**Figure 8.** Plot of initial rate of anhydride (**4**) arylation versus the concentration of Ph₂Zn: [Ni(COD)₂] = 7.4 mM, [bipy] = 8.0 mM, [4-fluorostyrene] = 16 mM, [4] = 0.10 M at 0 °C.**Table 1.** Effects of Olefin Additives in the Yield and Enantioselectivity of the Desymmetrization of **8** with Et₂Zn, Catalyzed by Ni(COD)₂ and ⁱPrPHOX^a

Entry	Additive	Yield (%)	ee ^b (%)
1	R = <i>p</i> -F	93	61
2	R = <i>m</i> -F	86	56
3	R = <i>o</i> -F	80	44
4	R = H	92	63
5		40	<10
6		70	18
7		<20	<10
8		<15	10
9	none	77	4

^a Reactions conducted in the presence of Ni(COD)₂ (10 mol %), ⁱPrPHOX (12 mol %), additive (20 mol %) and 1.2 equiv of Et₂Zn at 0 °C in THF for 14 h. ^b Enantiomeric excess determined by HPLC analysis of the corresponding benzyl ester.

philes, transmetalation serves as the turnover-limiting step, a result consistent with the comparative ease of sp²–sp² reductive elimination relative to that of sp²–sp³.²¹

Ni(COD)₂–ⁱPrPHOX System. In previous work, we identified ⁱPrPHOX²² as the most promising ligand for enantioselective anhydride alkylation with Et₂Zn.^{4a,6} In the presence of 4-fluorostyrene, at 0 °C, the desymmetrization of 4-methylglutaric anhydride **8** provides ketoacid **9** in 93% yield and 61% ee (Scheme 7). During the course of optimizing reaction conditions, it was observed that in addition to the yields and reaction times, the identity of the styrenic additive affects the enantioselectivity of the transformation. To further examine this phenomenon, we extended our use of additives to other olefins. The results of this screen are shown in Table 1.

Whereas the qualitative effect of the olefinic additives is similar to that observed in the Ni(COD)₂–bipy system described above, the observation of a change in enantioselectivity indicates the role of the olefin must be more significant than prevention of decomposition. In light of this evidence of styrene participation, as well as our interest in further developing the enantioselective reaction, we began a second study to determine the role of styrene in the Ni(COD)₂–ⁱPrPHOX-catalyzed cycle and

(21) Brown, J. M.; Cooley, N. A. *Chem. Rev.* **1988**, *88*, 1031 and references therein.

(22) Helmchen, G.; Pfaltz, A. *Acc. Chem. Res.* **2000**, *33*, 336.

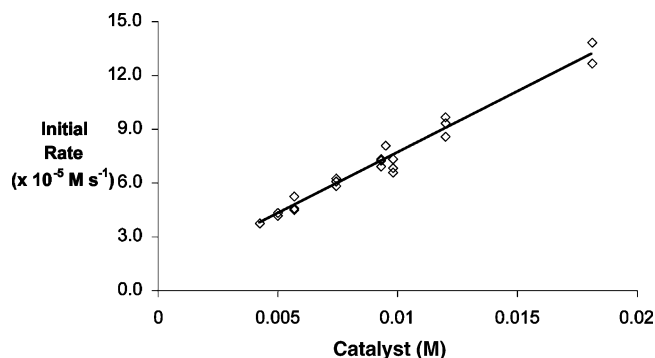


Figure 9. Plot of initial rate of the alkylation of **8** versus catalyst concentration (1:1.1 ratio of Ni(COD)₂/ⁱPrPHOX): [**8**] = 0.11 M, [Et₂Zn] = 0.16 M, [styrene] = 0.032 M at 23 °C.

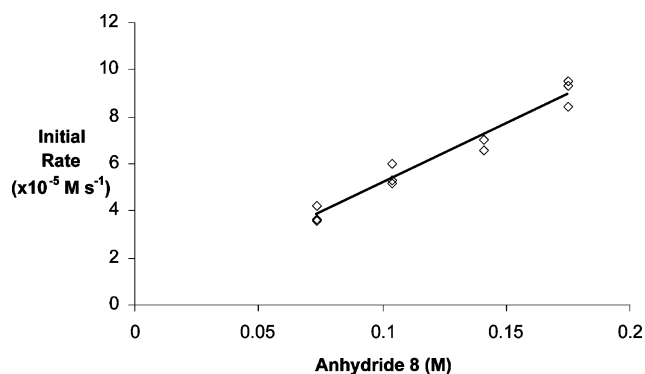


Figure 10. Plot of initial rate versus anhydride concentration for the alkylation of 4-methylglutaric anhydride **8**: [Ni(COD)₂] = 6.5 mM, [ⁱPrPHOX] = 7.2 mM, [Et₂Zn] = 0.16 M, [styrene] = 0.032 M at 23 °C.

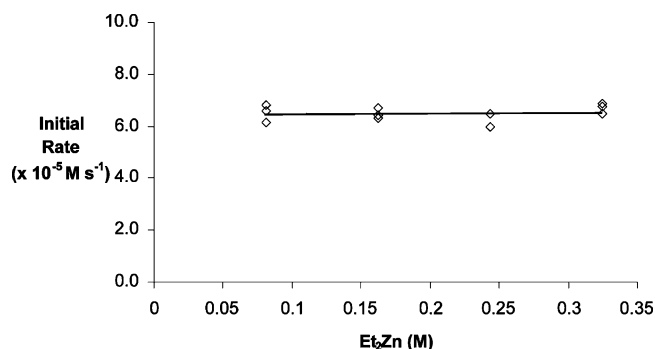


Figure 11. Plot of initial rate versus Et₂Zn concentration for the alkylation of 4-methylglutaric anhydride **8**: [**8**] = 0.11 M, [Ni(COD)₂] = 6.5 mM, [ⁱPrPHOX] = 7.2 mM, [styrene] = 0.032 M at 23 °C.

identify other differences between the Ni–bipy and Ni–ⁱPrPHOX cycles.

Kinetics of Ni(COD)₂–ⁱPrPHOX System. The study was carried out at room temperature utilizing 4-methylglutaric anhydride (**8**) in the presence of Ni(COD)₂, ⁱPrPHOX, and styrene, with Et₂Zn as the alkylating agent (Scheme 6). Kinetic analysis, again utilizing the method of initial rates, revealed first-order rate dependence upon the concentration of catalyst and anhydride (Figures 9 and 10). In contrast to the earlier study, the reaction rate displays zero-order dependence upon Et₂Zn concentration (Figure 11). Variation of styrene concentration results in saturation behavior of the reaction, which proceeds with an initial rate of $2.2 \times 10^{-5} \text{ M s}^{-1}$ in the absence of styrene and accelerates with increasing styrene concentration, plateauing at approximately $8.0 \times 10^{-5} \text{ M s}^{-1}$ above 0.03 M styrene (Figure 12).

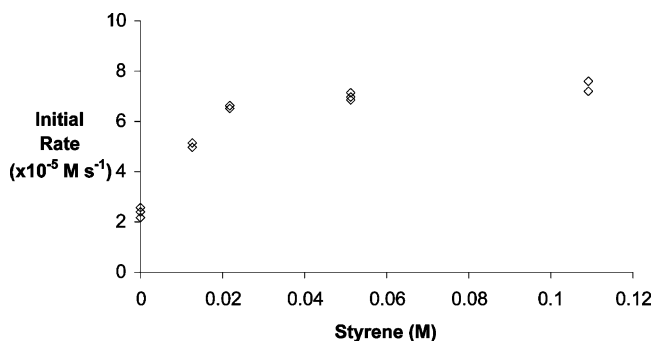
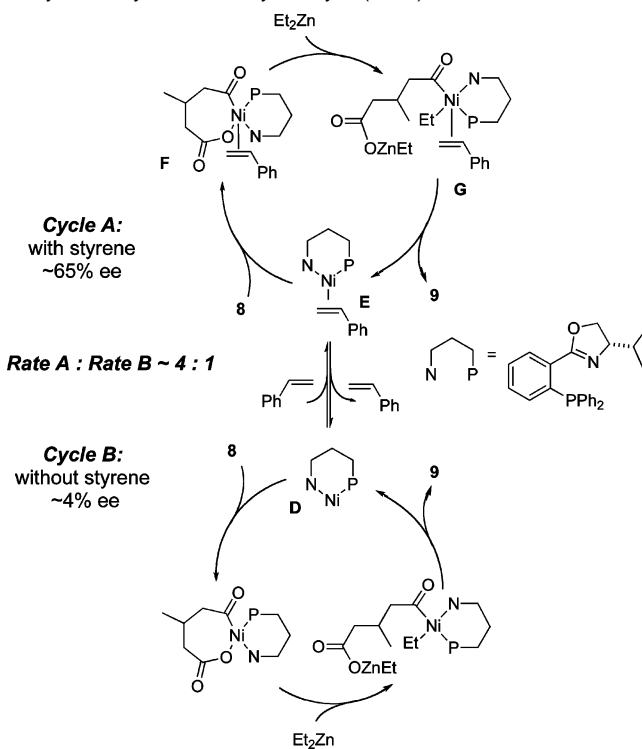


Figure 12. Plot of initial rate versus styrene concentration for the alkylation of 4-methylglutaric anhydride **8**: [**8**] = 0.11 M, [Ni(COD)₂] = 6.5 mM, [ⁱPrPHOX] = 7.2 mM, [Et₂Zn] = 0.16 M at 23 °C.

Scheme 8. Proposed Dual Catalytic Cycle for Alkylation of Anhydrides by Et₂Zn Catalyzed by Ni(COD)₂ and ⁱPrPHOX



These data suggests a significant change in the relative rates of processes within the catalytic cycle from those observed in the Ni(COD)₂–bipy system. First-order rate dependence upon anhydride suggests that oxidative addition is turnover limiting, which effectively hides the nature of the following steps. In addition, the nonzero rate at 0 M styrene suggests the presence of two separate catalytic cycles: a fast cycle in the presence of styrene and a slow cycle in its absence. Scheme 8 depicts a proposed dual catalytic cycle consistent with the kinetic results.

The enantioselectivity of the alkylation of **8** with Et₂Zn also displays saturation behavior with increasing styrene concentration. In the absence of styrene, the enantioselectivity of the product ketoacid is only 4% but increases with styrene concentration, plateauing at 65% at concentrations >0.06 M (Figure 13). This observation provides further credence for the two-cycle mechanism. The slow cycle without styrene, provides the ketoacid in 4% ee, while the cycle with styrene proceeds significantly faster and provides the product in approximately

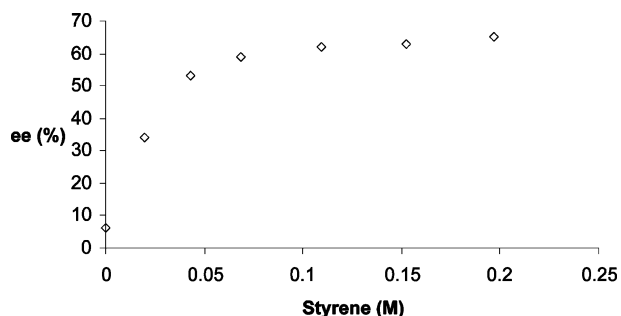
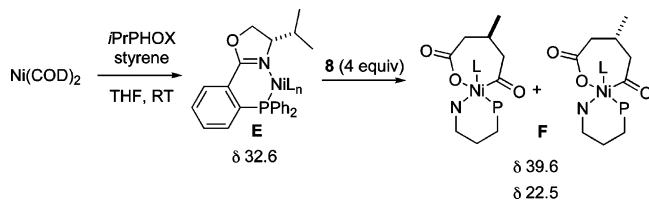


Figure 13. Plot of enantioselectivity versus styrene concentration: $[\text{Ni}(\text{COD})_2] = 6.5 \text{ mM}$, $[\textit{i}\text{PrPHOX}] = 7.2 \text{ mM}$, $[\mathbf{8}] = 0.10 \text{ M}$, $[\text{Et}_2\text{Zn}] = 0.16 \text{ M}$ at $23 \text{ }^\circ\text{C}$.

Scheme 9. ^{31}P NMR Investigation of Catalytic Intermediates

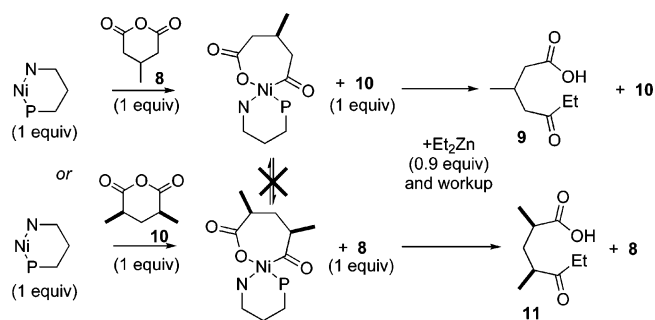


65% ee. The predominant cycle is dictated by the concentration of styrene in the system.

Investigation of Resting State. This reaction was also examined utilizing ^{31}P NMR spectroscopy in order to observe the resting state of catalysis. The stoichiometric reaction of $\textit{i}\text{PrPHOX}$ with $\text{Ni}(\text{COD})_2$ with 2 equiv of styrene resulted in a new species with a ^{31}P NMR resonance at $\delta 32.6 \text{ ppm}$, tentatively assigned as **E**. The ^{31}P NMR spectrum of the product of addition of a slight excess of 4-methylglutaric anhydride **8** revealed two new resonances at $\delta 39.6$ and 22.5 (Scheme 9).²³ These resonances, observed in a 2:1 ratio, are presumably due to diastereomers. It should be noted that, although numerous diastereomers are possible, particularly with consideration of styrene coordination and metal geometry, only two are observed. One of these diastereomers corresponds to **F**, the intermediate resulting in the formation of the major enantiomer of product.

Finally, a ^{31}P NMR spectrum of a catalytically active solution was obtained. At approximately 50% consumption of anhydride **8**, the only ^{31}P NMR resonance observed was $\delta 32.6$, consistent with intermediate **E**, as assigned by the stoichiometric experiments. These results suggest that intermediate **E** is the resting state of catalysis, a result that is consistent with turnover-limiting oxidative addition (Scheme 8).

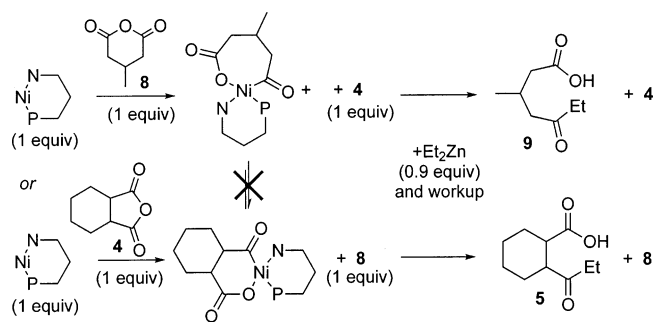
Irreversible Oxidative Addition. The reversibility of oxidative addition in the $\text{Ni}(\text{COD})_2$ - $\textit{i}\text{PrPHOX}$ system was tested in a manner identical to that described for the $\text{Ni}(\text{COD})_2$ -bipy system (Figure 6). The oxidative addition product was formed using anhydride **8** with a stoichiometric amount of $\text{Ni}(\text{COD})_2$ and $\textit{i}\text{PrPHOX}$, with 2 equiv of styrene (Figure 14). Addition of 3,5-dimethylglutaric anhydride (**10**) was closely followed by addition of Et_2Zn . Analysis of the product mixture revealed a greater than 10:1 ratio favoring **9**, the alkylation product of **8**, a result which suggests that oxidative addition is irreversible. To ensure that this ratio was due to irreversible oxidative addition and not a result of an equilibrium, the order of addition was reversed. Formation of the oxidative addition complex of **10** was followed by addition of **8** and Et_2Zn . Workup and



8 followed by **10** provides **9:11** in >10:1 ratio

10 followed by **8** provides **9:11** in <1:10 ratio

Figure 14. Oxidative addition reversibility experiment with Ni - $\textit{i}\text{PrPHOX}$ and two glutaric anhydrides.



8 followed by **4** provides **9:5** in >10:1 ratio

4 followed by **8** provides **9:5** in <1:10 ratio

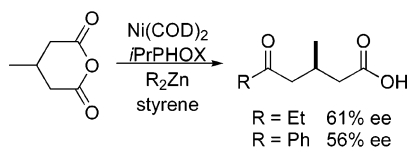
Figure 15. Oxidative addition reversibility experiment with Ni - $\textit{i}\text{PrPHOX}$ and structurally different anhydrides.

analysis again revealed a greater than 10:1 ratio favoring **11**, the alkylation product of **10**, which was first added to the $\text{Ni}(\text{COD})_2$ - $\textit{i}\text{PrPHOX}$ complex. These results provide conclusive evidence for irreversible anhydride oxidative addition.

To ensure that the differing catalytic cycles are a result of the ligands rather than the anhydrides, the reversibility experiments described above were repeated in a crossover manner using succinic anhydride **4** and glutaric anhydride **8** (Figure 15). In each case, the initially reacted anhydride was alkylated with nearly complete selectivity over the second anhydride, indicating that oxidative addition is irreversible for both glutaric and succinic anhydrides in the Ni - $\textit{i}\text{PrPHOX}$ -catalyzed alkylation. These results suggest that the slight variation in mechanism between the Ni -bipy- and Ni - $\textit{i}\text{PrPHOX}$ -catalyzed reactions is a product of the electronic influence of the ligand on the identity and stability of the catalytic resting state.

The proposed catalytic cycle for anhydride alkylation catalyzed by $\text{Ni}(\text{COD})_2$ and $\textit{i}\text{PrPHOX}$ predicts that, as anhydride oxidative addition is the turnover-limiting step, the rate and enantioselectivity of ketoacid formation should be independent of the zinc reagent. Under high styrene concentration (0.062 M), the alkylation of **8** was performed using Ph_2Zn (Scheme 10). As predicted, the reaction rate, $5.88 \times 10^{-5} \text{ M s}^{-1}$, and enantioselectivity, 56% ee, were similar to those obtained using Et_2Zn under identical conditions ($5.68 \times 10^{-5} \text{ M s}^{-1}$ and 61% ee). This observation, consistent with that predicted, provides evidence that oxidative addition is the rate-limiting and enantioselectivity-determining step.

(23) See Supporting Information for full reaction details and ^{31}P NMR spectra.

Scheme 10. Comparison of Alkylation of **8** with Ph_2Zn and Et_2Zn 

Ni(COD)₂-ⁱPrPHOX Mechanism. The catalytic cycle proposed for the Ni-ⁱPrPHOX catalyzed alkylation involves several notable factors, primarily focusing upon the role of styrene. Rather than influencing reductive elimination, as is observed in stoichiometric studies²⁴ and hypothesized in catalytic cross-coupling reactions,^{8,10} the presence of styrene impacts the oxidative addition step. This is somewhat counterintuitive as one might expect that coordination of an electron-deficient styrene should slow oxidative addition rather than accelerate this process. Furthermore, the variation in enantioselectivity with the nature of the styrene indicates that the styrene is present during the enantioselectivity-determining step. One potential reason for this situation may be the inherent difference between a bidentate COD vs monodentate styrene ligand on nickel. For steric or electronic reasons, ⁱPrPHOX-Ni prefers to ligate styrene over COD, thereby creating a three-coordinate Ni(0) complex with a vacant coordination site to accommodate the anhydride. The corresponding four-coordinate ⁱPrPHOX-NiCOD complex would require olefin dissociation to form the more active three-coordinate species, which, by definition, would be present in low concentration having the pendent olefin ligand in proximity.

Conclusion

The kinetic study of these catalyst systems has provided several notable insights. Analysis of the Ni(COD)₂-bipy system

- (24) (a) Yamamoto, T.; Yamamoto, A.; Ikeda, S. *J. Am. Chem. Soc.* **1971**, *93*, 3350. (b) Sustmann, R.; Lau, J.; Zipp, M. *Tetrahedron Lett.* **1986**, *27*, 5207. (c) Sustmann, R.; Hopp, P.; Holl, P. *Tetrahedron Lett.* **1989**, *30*, 689.

has revealed turnover limiting reductive elimination at high Et₂Zn concentration, an unusual occurrence for carbon-carbon cross-coupling. We have also observed two significantly different roles for styrene. Although our results support the qualitative observations of more facile cross-coupling in the presence of styrene, alternate rationale for such improvement has been provided. Rather than assisting in reductive elimination, styrene appears to influence catalyst stability and oxidative addition in these two systems. In Ni-bipy-catalyzed alkylation, the presence of 4-fluorostyrene inhibits catalyst decomposition and provides higher yields at long reaction times, yet has no effect on the initial rate of reaction. In contrast, Ni-ⁱPrPHOX-catalyzed alkylation proceeds via competing catalytic cycles differentiated by the presence of styrene. Through a mechanism that is not fully understood, the presence of styrene accelerates oxidative addition and promotes a catalytic cycle that proceeds more rapidly and with higher selectivity than its styrene-lacking analogue. These results promise to impact the rational development of new systems capable of catalyzing anhydride alkylation and to influence other cross-coupling reactions.¹⁰

Acknowledgment. T.R. thanks Johnson and Johnson, Merck, Eli Lilly and Boehringer-Ingelheim for support. T.R. thanks the Monfort Family Foundation for a Monfort Professorship. T.R. is a fellow of the Alfred P. Sloan Foundation. J.B.J. thanks the NIH for a postdoctoral fellowship. G.W.C. gratefully acknowledges funding from the NSF (CHE-0243605) and DOE (DE-FG02-05ER15687).

Supporting Information Available: Experimental procedures, including spectral and kinetic data. This material is available free of charge via the Internet at <http://pubs.acs.org>.

JA067845G